Journal of Catalysis 356 (2017) 14–21

Contents lists available at ScienceDirect

Journal of Catalysis

journal homepage: www.elsevier.com/locate/jcat

Electrochemical production of lactic acid from glycerol oxidation catalyzed by AuPt nanoparticles

Chencheng Dai [a,b], Libo Sun [b,f], Hanbin Liao [a], Bahareh Khezri [b,g], Richard D. Webster [b,g], Adrian C. Fisher [b,e], Zhichuan J. Xu [a,b,c,d,*]

[a] School of Material Science and Engineering, Nanyang Technological University, 50 Nanyang Avenue, Singapore 639798, Singapore
[b] The Cambridge Centre for Advanced Research and Education in Singapore, 1 CREATE way, Singapore 138602, Singapore
[c] Solar Fuels Laboratory, Nanyang Technological University, 50 Nanyang Avenue, Singapore 639798, Singapore
[d] Energy Research Institute @ Nanyang Technological University, 50 Nanyang Avenue, Singapore 639798, Singapore
[e] Department of Chemical Engineering and Biotechnology, University of Cambridge, New Museum Site, Pembroke Street, Cambridge CB2 3RA, UK
[f] School of Chemical and Biomedical Engineering, Nanyang Technological University, 62 Nanyang Drive, Singapore 637459, Singapore
[g] Division of Chemistry & Biological Chemistry, School of Physical Mathematical Sciences, Nanyang Technological University, 21 Nanyang Link, Singapore 637371, Singapore

ARTICLE INFO

Article history:
Received 29 July 2017
Revised 6 October 2017
Accepted 6 October 2017

Keywords:
Lactic acid
Glycerol oxidation
AuPt nanoparticles
Electro-oxidation
Alkaline

ABSTRACT

The production of valuable chemicals from relatively inexpensive feedstocks utilizing electrochemical methods has been attracting widespread attention in recent years since it is highly efficient, decentralized, environmental-friendly and can operate in room temperature and pressure. Currently, the industrial production of lactic acid is mainly based on bio-fermentation, leading to drawbacks including severe conditions, unfriendliness to environment, low efficiency and requirement of expensive equipment, which can potentially overcome by electrochemical methods. Herein, we report for the first time the preparation of lactic acid at room temperature and pressure from the one-pot electro-oxidation of glycerol, a byproduct from biodiesel production. AuPt nanoparticles with different surface compositions were employed in this work to optimize the catalysis performance, and the glycerol oxidation was operated at a series of applied potentials, pH and glycerol concentration. The optimal lactic acid selectivity was 73%, obtained with Au-enriched surface at applied potential of 0.45 V vs. RHE.

1. Introduction

Lactic acid (LA) is a valuable chemical utilized for the production of biodegradable poly(lactic acid) (PLA), polyester, as well as a feedstock for the synthesis of green solvents and various commodity chemicals [1,2]. In addition, LA is widely used directly in the pharmaceutical, food and detergent industries [1,2]. Until now, the production of LA is mainly based on fermentation of carbon sources, which has several disadvantages, such as severe conditions, unfriendliness to environment and low efficiency [3,4]. The demand for LA has been estimated to grow yearly at 5–8% and been forecast to reach 367,300 metric tons by the year 2017[5]. One of the cheapest sources for LA is glycerol, a major byproduct from biomass conversion and soap manufacturing [6,7]. The global glycerol market size was 2.47 million tons in 2014 and is expected to increase 6.5% from 2015 to 2022 annually [8]. The market price of refinery glycerol (99.5%) is only approximately 500 USD/tons [9]. The production of LA from glycerol has been reported mainly using the hydrothermal [10–14] and hydrogenolysis methods, [15–17] with Au, Pt and their bimetallic catalysts frequently used for such methods [12–14,17]. Nevertheless, these methods typically suffer from severe drawbacks including requirement of expensive equipment and high energy input (such as high reaction temperature and pressure).

Electrochemical methods are often regarded as green processes because of their high energy efficiency in converting chemicals with electrons. Compared with the hydrothermal and hydrogenolysis methods, electrochemistry allows low reaction temperature and pressure due to the non-thermal activation in aqueous media. Additionally, the control of the applied potential, the solution pH, the glycerol concentration and the formulation of catalysts are expected to allow the tuning of the selectivity and activity of the oxidation reaction. The electrochemical oxidation of glycerol has been studied using a list of catalysts, such as Pt, Au, and a range of metals and metal oxides [18–25].

* Corresponding author at: School of Material Science and Engineering, Nanyang Technological University, 50 Nanyang Avenue, Singapore 639798, Singapore.
E-mail address: xuzc@ntu.edu.sg (Z.J. Xu).

https://doi.org/10.1016/j.jcat.2017.10.010
0021-9517/

Pt is considered as the reference material for the electro-oxidation of alcohols in both acidic and alkaline media [18,23,24]. Kwon et al. [18] studied the mechanism and selectivity of glycerol oxidation on polycrystalline Pt employing an online measurement. They found that on Pt, glyceric acid (GLA) produced via oxidation of glyceraldehyde (GLAD) starting from 0.4 V vs. RHE was the main product in alkaline media, and as the pH was decreased GLAD became the main product. Other low concentration products also included dihydroxyacetone (DHA), hydroxypyruvic acid (HA), glycolic acid (GA), formic acid (FA), oxalic acid (OA), and tartronic acid (TA). Roquet et al. [24] studied the electro-oxidation of glycerol on platinum electrodes during long-term potential-controlled electrolysis. The product selectivity and conversion rate were found to depend greatly on the applied potential and on the pH of the electrolyte. They also found that in alkaline media the reaction kinetics were globally higher, and the adsorption and oxidation of glycerol with C—C bond cleavage appeared limited.

Au is inactive in acidic media for alcohol oxidation, while the surface becomes more active in alkaline media [18,23]. Kwon et al. [18] also studied the glycerol electro-oxidation on polycrystalline Au electrodes in alkaline media using an online method. They observed only three products, GA, FA and GLA. The GLA was detected first at 0.8 V vs. RHE instead of GLAD, which indicated the rapid oxidation from glycerol to GLA via glyceraldehyde, primarily due to the higher overpotential applicable to Au. This product was further oxidized at higher potential to form GA and FA. Wang et al. [21] prepared Au nanoparticles supported on extended poly(4-vinylpyridine) functionalized graphene. The products obtained from chronoamperometry at 0.2 V vs. Hg/HgO in alkaline media were mainly composed of GLA, with byproducts including FA, GA, OA and TA. Qi et al. [25] investigated the electro-oxidation of glycerol on Au in anion exchange membrane-direct glycerol fuel cells. Byproducts of the reaction after 12 h included mesoxalic acid (MA), GLA, GA, TA, OA with a minimal amount of LA (less than 10%). It should also be noted that during the preparation of this manuscript, Lam et al. reported the production of LA from glycerol electro-oxidation catalyzed by cobalt-based catalyst [26]. However, the highest selectivity towards LA is only 37% even in 3 M NaOH at 60 °C, and the selectivity towards LA is only 7% at room temperature. Regretfully, none of the reports on the electro-oxidation of glycerol have observed a major production of LA at room temperature and pressure using either online or offline measurement.

Herein, we report the electrochemical preparation of LA from glycerol at room temperature and pressure for the first time. AuPt bimetallic nanoparticles were prepared as catalysts. Since there has been no attempt to use AuPt for catalyzing the glycerol electro-oxidation so far, the AuPt synergetic effect on glycerol electro-oxidation was studied by comparing the performance of AuPt nanoparticles with different surface compositions and analyzing the corresponding oxidation products. Moreover, the influence of reaction parameters, including applied potential, glycerol concentration, solution pH, and reaction time, on the product selectivity, glycerol conversion and Faradaic efficiency was also investigated. Noticeably, different from the product compositions reported of glycerol oxidation on Au or Pt electrodes previously, the AuPt nanoparticles in this work exhibited LA selectivity as high as 73% under the optimal conditions.

2. Experimental details

2.1. Reagents

Dihydroxyacetone was purchased from Merck, glyceric acid was purchased from TCI, and all other chemicals were purchased from Sigma-Aldrich. All the chemicals were used without further purification. Solutions were prepared with deionized water and had resistivity no less than 18.2 MΩ·cm at 25 °C from Millipore Milli-Q.

2.2. Nanoparticle synthesis and electrode preparation

AuPt bimetallic nanoparticles were synthesized by modifying the method reported by Gaw et al. [27]. 0.25 mmol $HAuCl_4$ and 0.25 mmol $Pt(acac)_2$ were dissolved in 20 mL oleylamine. The solution was heated to 160 °C and maintained at this temperature for 2 h under argon blanket. Afterward, 100 mL ethanol was added and the mixture was centrifuged at 8000 rpm for 10 min. The resulted sediment was by the mixture of hexane and ethanol through centrifuging at 8000 rpm for 10 min for 3 times. The final sediment/nanoparticles was/were loaded to the Vulcan CX72 carbon support with a mass loading approximate 20 wt% by sonicating the mixture of nanoparticles and carbon in hexane in an ice bath for 3 h. The catalyst powders were then collected by purging Ar at room temperature and dried in vacuum. The catalyst ink (4 mg/ml) was prepared by mixing the catalyst with DI water/IPA/Nafion solution at a volume ratio of 4:1:0.2. The mixture was ultrasonicated in an ice bath for 1 h before dropped onto the carbon substrate.

2.3. Heat treatment of AuPt nanoparticles

The heat treatment of as-synthesized AuPt (90% Pt_{surf})/C was carried out in a tube furnace (Lindberg/Blue M) using a quartz tube, and it followed the method reported by Suntivich et al. [28]. Three types of AuPt/C with different surface compositions were prepared. (1) AuPt/C with surface composition of 64% Pt: Approximately 40 mg AuPt (90% Pt_{surf})/C was placed in a tube furnace, and purged with dry air at a flow rate of 100 mL/min. The tube furnace was heated up to 250 °C with a heating rate of 5 K/min, and maintained at this temperature for 30 min. Afterward, the tube furnace was allowed to naturally cool down to room temperature. (2) AuPt/C with surface composition of 29% Pt: Approximately 40 mg AuPt (90% Pt_{surf})/C was placed in a tube furnace, and purged with dry air at a flow rate of 100 mL/min. The tube furnace was heated up to 250 °C with a heating rate of 5 K/min, and maintained at this temperature for 30 min. Then the dry air was replaced by argon with the same flow rate. The temperature was further raised up to 350 °C with the same heating rate, and the temperature was maintained for another 30 min. Afterward, the tube furnace was allowed to naturally cool down to room temperature. (3) AuPt/C with surface composition of 15% Pt: Approximately 40 mg AuPt (90% Pt_{surf})/C was placed in a tube furnace, and purged with argon at a flow rate of 100 mL/min. The tube furnace was heated up to 500 °C with a heating rate of 5 K/min, and maintained at this temperature for 30 min. Afterward, the tube furnace was allowed to naturally cool down to room temperature.

2.4. Characterizations of AuPt nanoparticles

The surface composition was determined based on the electrochemical methods reported [27,28]. The electrochemical surface areas (ESAs) of Au and Pt in 0.5 M H_2SO_4 were measured by cyclic voltammetry utilizing a three-electrode system with a Hg/Hg_2SO_4 (sat. K_2SO_4) reference electrode and a graphite counter electrode, with Ar bubbling. The potential applied ranged from 0.05 V to 1.7 V vs. RHE at a scan rate of 50 mV/s. All electrochemical measurements were controlled by a PGSTAT30 Autolab potentiostat (Ecochemie). The particle size distribution was measured by a JEOL 2010 transmission electron microscope (TEM) at the operating voltage of 200 kV. Powder X-ray diffraction (PXRD) pattern measurements were recorded using a Shimadzu Thin Film X-ray

diffractometer (Cu Kα radiation, λ = 0.154 nm). The diffractometer operating conditions were 40 kV, 30 mA at a 2q range of 10–80 with the scan speed of 3° min^{-1}. Thermogravimetric analysis (TGA) of AuPt/C nanoparticles was carried in a TGA/DSC 2 STAR System (Mettler Toledo). AuPt/C nanoparticles were heated from 25 °C to 800 °C in air with a heating rate of 10 K/min. Trace metal analysis of AuPt/C nanoparticles was performed using an Agilent 7700x ICP-MS (Agilent Technologies). Samples were digested using Milestone Ethos one microwave digestion system before the analysis.

2.5. Electrochemical oxidation of glycerol

The electrochemical oxidation of glycerol was performed in an H-type cell utilizing a three-electrode system with a Hg/HgO (1 M KOH) reference electrode and a graphite counter electrode (schematic illustration shown in Fig. 1a). The two compartments were separated with an AMI-7001 anion exchange membrane (Membranes International), and the counter electrode was separated from the working and reference electrodes to prevent the reduction of oxidation products at the counter electrode. The membrane was immersed in the 1 M KOH solution overnight before the test. Glycerol (0.5 M) was dissolved into a 1 M KOH solution (or other concentrations when mentioned), and the solution was bubbled with Ar to purge air before and during experiments. Each chamber was filled with 10 mL of 0.5 M glycerol & 1 M KOH solution. A graphite paper (20 mm × 15 mm) with AuPt nanoparticles loading of 120 μg/cm^2 on both sides was used as the working electrode. The reaction products were collected with a syringe at fixed time during or after chronoamperometry tests for the following product analysis. The catholyte was also analyzed after electrolysis, and no electro-oxidation product was detected using either NMR or HPLC methods.

2.6. Analysis of glycerol oxidation products

Chromatographic determination of glycerol oxidation products was analyzed by an Agilent 1260 Infinity II HPLC (Agilent Technologies). The column used was an Aminex HPX87-H (Bio-Rad) and the eluent used was 5 mM sulfuric acid. During the test, 20 μL mixture of 0.5 M H_2SO_4 and sample solution was injected into the column and the temperature of the column was kept at 55 °C. The flow rate was 0.5 mL/min. The separated compounds were detected with a refractive index detector (RID) and a multiple wavelength detector (MWD). The expected products were also analyzed by HPLC to perform a standard calibration curve. Both ^{1}H-NMR and ^{13}C-NMR spectrum were recorded using a Bruker AV 300 MHz NMR spectrometer. 0.4 mL sample and 0.2 mL D_2O were mixed and used for each test.

3. Results and discussion

3.1. Catalyst characterizations

The as-synthesized and heat-treated AuPt nanoparticles were first electrochemically characterized to determine the surface composition [27,28]. All potentials mentioned are vs. RHE, for simplicity and comparison. Fig. S1 shows CVs of AuPt nanoparticles with different surface compositions. The ESA of Pt was calculated by integrating and averaging the capacity-corrected by hydrogen underpotential adsorption/desorption in the range of 0.05 – 0.4 V using the constant of 210 μC/cm^2. The ESA of Au was calculated by integrating the reduction peak of gold oxide in the range from ca. 0.95 V to 1.3 V using the constant of 340 μC/cm^2. The AuPt (90% Pt_{surf}) nanoparticles possessed a Pt-rich surface (90 atom% Pt). Due to the lower surface energy of gold, higher surface Au compositions were induced according to the methods mentioned above, from AuPt (64% Pt_{surf}) with 64 atom% Pt, to AuPt (29% Pt_{surf}) with 29 atom% Pt and AuPt (15% Pt_{surf}) with 15 atom% Pt. This change in the composition converted a Pt-rich surface to an Au-rich surface. Fig. 1b&c and S2 shows the representative TEM images and particle size distribution of as-synthesized AuPt (90% Pt_{surf}) nanoparticles, respectively. The particle size was found to be 6.3 ± 1.4 nm. This observation is in accordance with the previous work by Suntivich et al. [28], in which AuPt nanoparticles with different surface compositions prepared by the same method have a particle size range of 6–8 nm. As for size effect of carbon-supported metal nanoparticles on electrochemical performance, normally it can be observed for those particles with more significant size difference [29,30]. Therefore, in such a small size variation range, the size effect of AuPt nanoparticles is limited. Fig. S3 shows the XRD analysis used to determine the structure of AuPt nanoparticles, and no phase separation was detected. The loading of AuPt nanoparticles on carbon was confirmed by the TGA tests, which was approximately 20 wt% (shown in Fig. S4). The molar ratio of Pt/Au calculated based on counts from ICP-MS for AuPt (90% Pt_{surf}), AuPt (64% Pt_{surf}), AuPt (29% Pt_{surf}) and AuPt (15% Pt_{surf}) were 1.05, 1.06, 1.03 and 1.04, respectively (shown in Table S1).

3.2. Product analysis and reaction pathways

To compare the influence of the AuPt surface composition and applied potential on the selectivity (molar percentage) and activity of the glycerol oxidation (total electron transferred), the glycerol oxidation was first operated at four different potentials, 0.45 V, 0.6 V, 0.9 V and 1.05 V, catalyzed by four types of as-synthesized AuPt nanoparticles for 12 h. The potentials were selected from the potential where the oxidation started for all AuPt catalysts in the linear sweep voltammetry (LSV) (shown in Figs. 2a and S5), to the potential inducing the surface segregation [27] and Pt dissolution [31]. Ar was bubbled during the whole reaction process to purge air, as lower O_2 concentration favors the formation of LA from glycerol oxidation [12,13]. The Au and Pt monometallic nanoparticles were also employed for comparison purpose. However, the glycerol oxidation over Au electrode was only performed at 0.9 V and 1.05 V, as the oxidation of glycerol on Au was only observed at potential higher than 0.6 V [32].

In all reactions in alkaline conditions, the products were obtained as salts, but they were marked as the acid forms for simplicity and comparison. The products of glycerol electro-oxidation were first qualitatively determined by NMR and HPLC. Figs. 3a, b and 4 show the ^{1}H, ^{13}C NMR and HPLC analysis of oxidation products of 0.5 M glycerol in 1 M KOH by AuPt (15% Pt_{surf}) at 1.05 V after 12 h, respectively. Fig. 3a and b shows that the products analyzed from the NMR include FA, acetic acid (AA) (concentration too low to be detected in ^{13}C NMR), GA, GLA, LA, TA, OA (no proton in the salt form to be detected in ^{1}H NMR) and the reactant, glycerol. In Fig. 4, the peaks at the retention time of 7.701, 9.161, 12.555, 14.301, 14.741, 15.528, 16.315, and 17.858 min are attributed to OA, TA, GLA, GA, LA, glycerol, FA and AA, respectively. The types of products are consistent with the results obtained from NMR. In addition, since there are no aldehyde and ketone group detected in NMR, the possible peak overlapping with glyceraldehyde (GLAD) (12.887 min) and dihydroxyacetone (DHA) (15.650 min) can be ignored. Moreover, the all-acids production is more accessible for separation and purification compared with the mixture of acids and aldehydes/ketones for industrial applications [33].

On the basis of products analyzed from the NMR and HPLC results, the proposed reaction pathway for glycerol oxidation is shown in Scheme 1. Glycerol is first oxidized to GLAD or DHA by

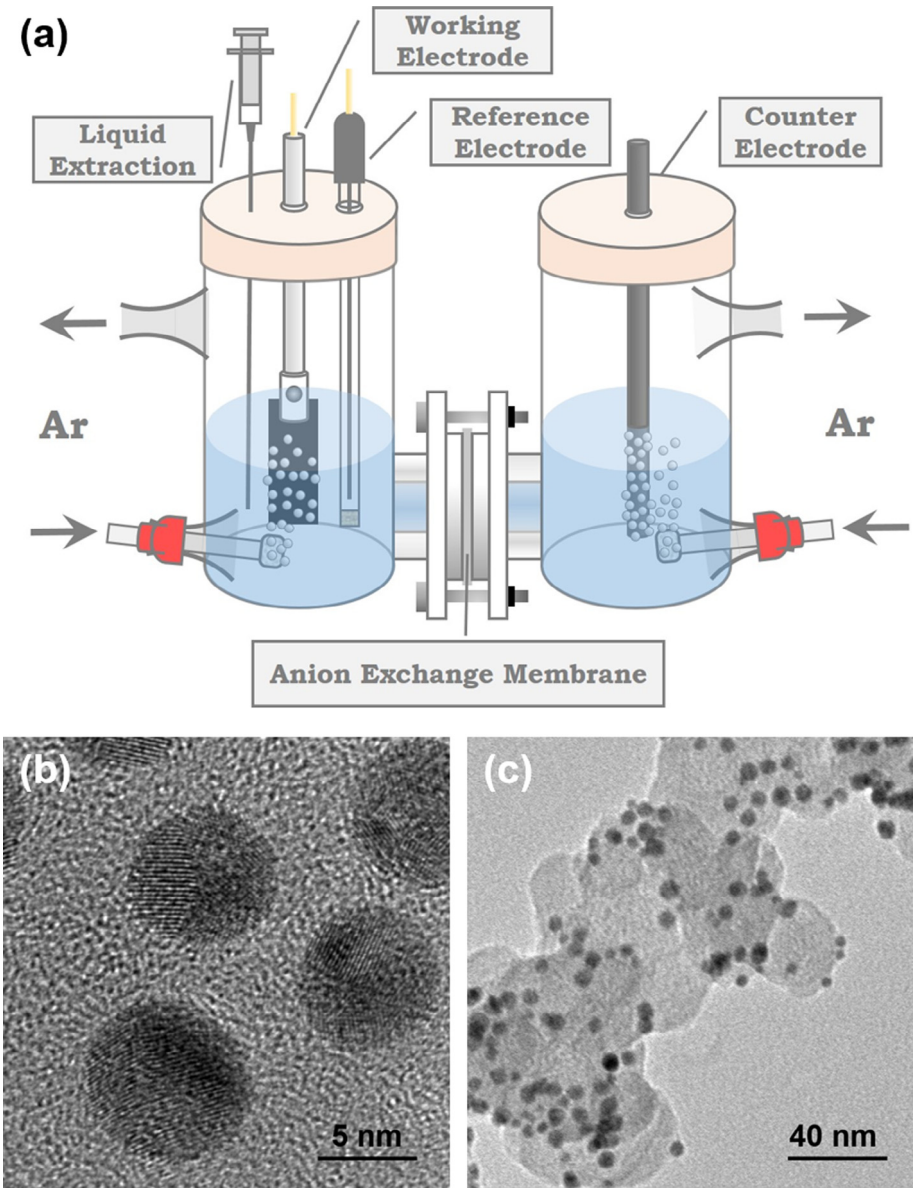

Fig. 1. (a) The schematic illustration of the electrochemical cell and three-electrode system used for glycerol oxidation; (b, c) representative TEM images of AuPt/C (90% Pt_{surf}) catalysts.

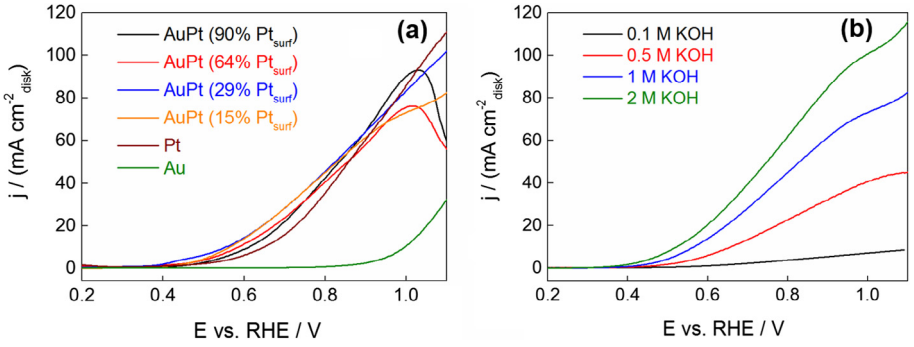

Fig. 2. Linear voltammograms of (a) glycerol oxidation catalyzed by different AuPt nanoparticles and Au & Pt nanoparticles in 0.5 M glycerol & 1 M KOH solution, and (b) glycerol oxidation catalyzed by AuPt (15% Pt_{surf}) in 0.5 M glycerol in KOH solutions of different concentrations. The plot represents the activity normalized by the electrode geometry area.

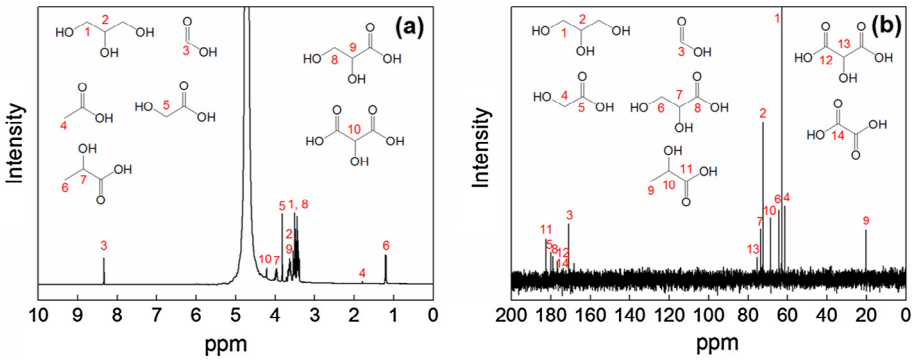

Fig. 3. (a) ^{1}H and (b) ^{13}C NMR spectra of the electrolyte solution after 12-h oxidation of glycerol on AuPt (15% Pt_{surf}) in 0.5 M glycerol & 1 M KOH solution at 1.05 V vs. RHE.

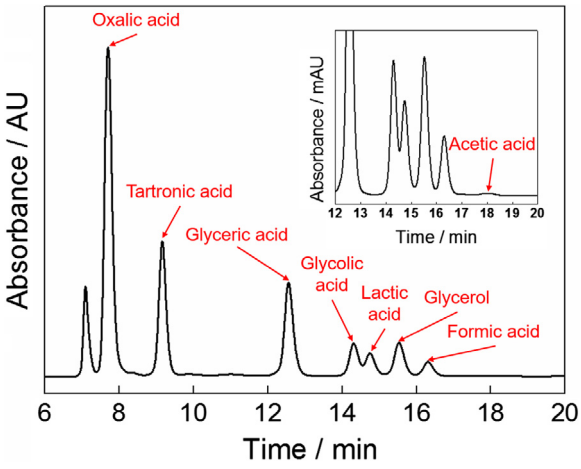

Fig. 4. HPLC chromatogram of the electrolyte solution after 12-h oxidation of glycerol on AuPt (15% Pt_{surf}) in 0.5 M glycerol & 1 M KOH solution at 1.05 V vs. RHE.

the coordination of AuPt catalyst and base. In this step, glycerol is first deprotonated (H_α in the R-CHH_β-OH_α) in the oxidation catalyzed by base, followed by the second deprotonation depending on the ability of the electrode material to abstract the H_β [34–36]. The resulting GLAD and DHA are in equilibrium in basic conditions [13]. They then undergo either base-catalyzed dehydration to 2-hydroxypropenal/pyruvaldehyde and followed with Cannizzaro rearrangement to LA, or further metal-catalyzed oxidation to GLA, TA, and C—C cleavage products such as GA, FA or OA (shown in Scheme 1) [12–14,18,26]. Since the pathways leading to LA and GLA are different and the pathway to GLA is undesired, an optimal catalyst/reaction parameter for the LA production therefore should have a strong oxidative dehydration capacity and at the same time being highly oxidatively inefficient for the conversion of GLAD/DHA into GA and subsequent products.

3.3. Catalyst and applied potential screening

The quantitative analysis of the products was performed by HPLC, and all results are summarized in Table S2. In Fig. 5, all AuPt catalysts demonstrated the same trend in that the lowest applied potential (0.45 V) resulted in the highest selectivity towards LA, although the glycerol conversion levels are the lowest. These results are consistent with the previous hypothesis of the reaction pathway. The lower applied potential leads to less oxidative activation to GLAD/DHA, which facilitate the reaction pathway following dehydration & rearrangement to LA and inhibits the reaction pathway to GLA and further oxidized products. Noticeably, the AuPt (90% Pt_{surf}) catalyst (shown in Fig. 5a) demonstrated selective tuning of product formation by the applied potential, from LA-dominant production (69% LA) at 0.45 V to GLA-dominant (53% GLA) production at 0.9 V. In addition, the highest GA & FA & OA production (33% GA, 9% FA and 3% OA), which represents the highest C2/C3 ratio, was achieved when using the AuPt (15% Pt_{surf}) catalyst with the applied potential of 1.05 V (shown in Fig. 5d). This indicates the highest C—C bond breaking capacity obtained in experiments. It is notable that the TA, which is also a high-value product [37], reached the highest selectivity when using the AuPt (64% Pt_{surf}) catalyst at a potential of 0.9 V (shown in Fig. 5b). This result suggests a technique for the production of such high-value chemical. In addition, the total concentration of all C3 and C2 products and remnant glycerol is very close to the original glycerol concentration. Therefore, other possible C3 and C2 products are ignorable, and the concentration of CO_2 (carbonate) is equal to the difference between total concentration of GA&OA and concentration of FA.

To measure the LA selectivity of different catalysts at 0.45 V, the performance of different AuPt and Pt catalysts was compared in Fig. 6a. The AuPt (15% Pt_{surf}) catalyst exhibited both the highest LA selectivity (73% LA) and glycerol conversion (0.295 ± 0.018). Meanwhile the AuPt (90% Pt_{surf}) catalyst displayed close LA selectivity (69% LA) while significantly smaller glycerol conversion (0.1608 ± 0.0116). The AuPt (64% Pt_{surf}) and AuPt (29% Pt_{surf}) catalysts demonstrated slightly smaller glycerol conversion (0.271 ± 0.013 and 0.288 ± 0.013, respectively), but distinct smaller LA selectivity (60% LA and 61% LA, respectively). Furthermore, the worst performance was obtained by the Pt catalyst, with the lowest LA selectivity (50% LA) and glycerol conversion level (0.107 ± 0.013).

To explain the trend in the LA selectivity and catalyst activity (based on the Faradaic current charge calculated from the product distribution and glycerol conversion), the AuPt catalyst with Pt-enriched surface was first considered. By comparing the performance of AuPt (90% Pt_{surf}) and AuPt (64% Pt_{surf}) catalysts, the LA selectivity decreased but catalyst activity increased (from 215 C to 396 C) with Au addition. The reason is that modification by Au on the Pt electronic structure is expected to promote the generation of OH_{ad} on the Pt surface and thus increase the alcohol oxidation capacity of the catalyst [38,39]. As a result, the Au increment increases the catalyst activity, and promotes the formation of GLA instead of LA from GLAD/DHA. Furthermore, to explain the increase in the LA selectivity and decrease in the catalyst activity of the AuPt (15% Pt_{surf}) catalyst compared with AuPt (29% Pt_{surf}), the Au surface enrichment leads to insufficient Pt for dehydrogenation of the alcohol, resulting in the negative contribution to the oxidation efficiency [27,28]. Consequently, the Au surface enrichment reduces the catalyst activity (from 426 C to 376 C), inhibits the GLA formation and facilitates the LA formation from GLAD/DHA. Moreover, the glycerol oxidation current at 0.45 V shown in Fig. 2a for AuPt catalysts follows the order AuPt (29% Pt_{surf}) > AuPt (64% Pt_{surf}) > AuPt (15% Pt_{surf}) > AuPt (90% Pt_{surf}), which is the

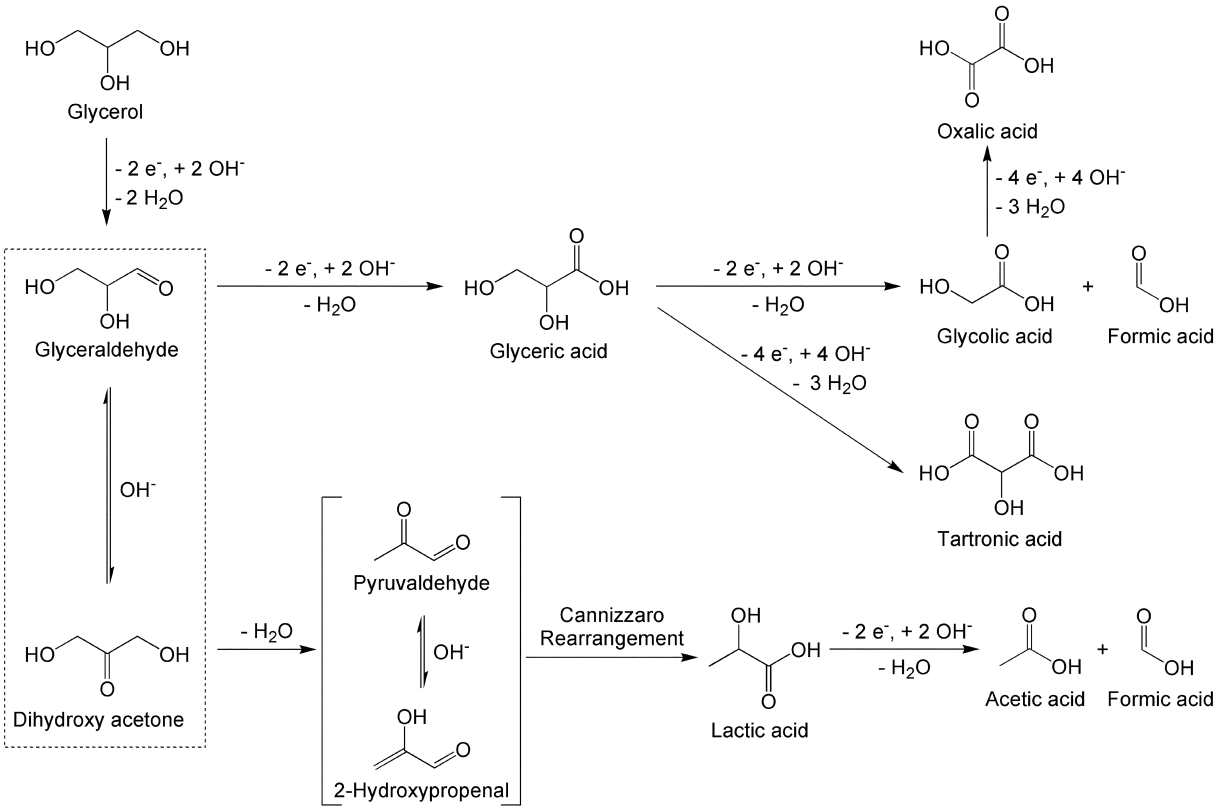

Scheme 1. Proposed reaction pathways for glycerol oxidation in alkaline solution on AuPt catalysts on the basis of products analyzed from NMR and HPLC.

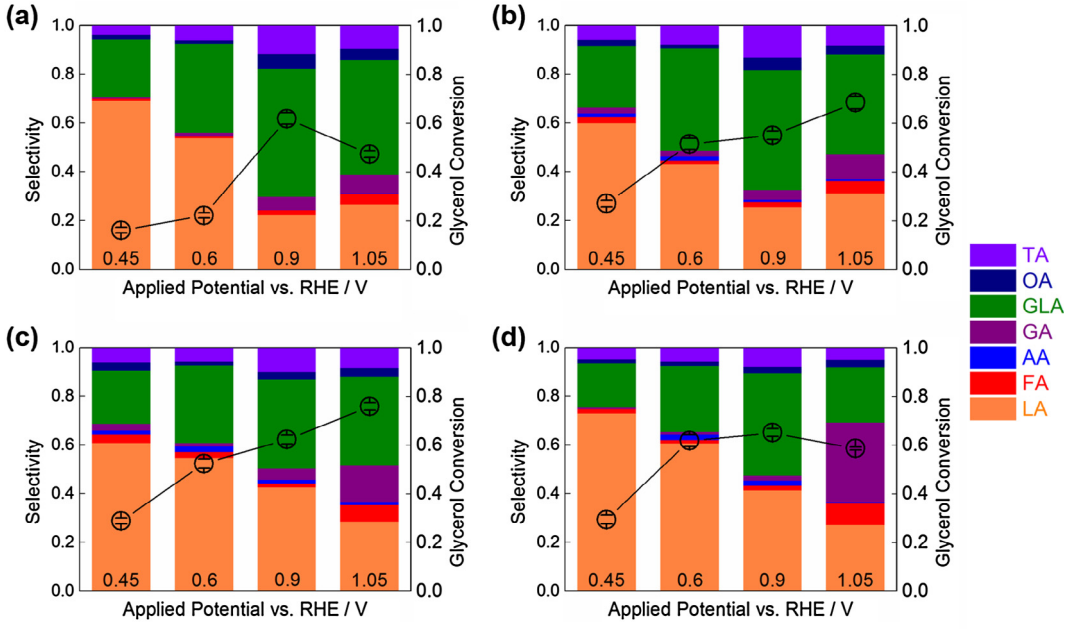

Fig. 5. Product distribution and glycerol conversion with different applied potentials over the (a) AuPt (90% Pt_{surf}), (b) AuPt (64% Pt_{surf}), (c) AuPt (29% Pt_{surf}), (d) AuPt (15% Pt_{surf}) catalysts in 0.5 M glycerol & 1 M KOH solution after 12 h.

congruent with the catalyst activities in glycerol oxidation chronoamperometry experiments. In addition, to explain the difference in LA selectivity between Pt monometallic catalyst and AuPt bimetallic catalysts, the reaction pathways on different metals are compared. Pt appears to favor the oxidation of the primary alcohol group to form GLAD, whereas Au allows the oxidation of the secondary alcohol group to form DHA [23,40]. Furthermore, Zhang et al. [14] reported that using DHA as the starting reagent led to a higher LA/GLA molar ratio compared with using GLAD as the starting reagent in the presence of base at low temperature of 15–140 °C. In addition, DHA or GLAD disappeared completely in 5 min of reaction time. Therefore, the AuPt catalysts facilitate the formation of a higher DHA/GLAD molar ratio and finally lead to higher LA selectivity, compared with Pt catalyst. Finally, to

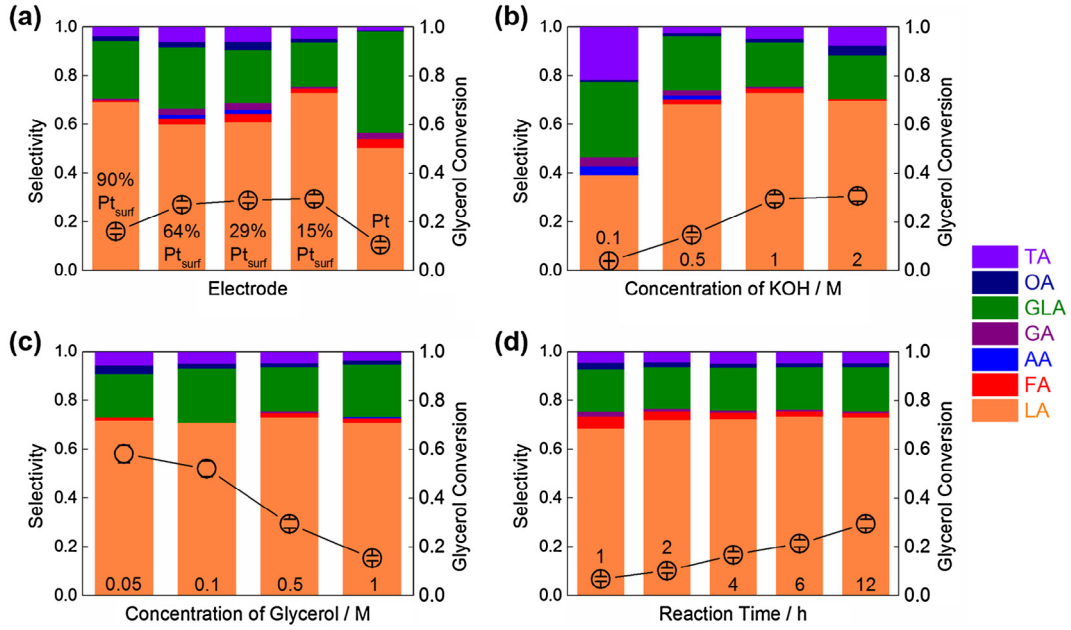

Fig. 6. Product distribution and glycerol conversion over the (a) AuPt and Pt electrodes with applied potential of 0.45 V vs. RHE after 12 h in 0.5 M glycerol and 1 M KOH solution; (b) AuPt (15% Pt_{surf}) with applied potential of 0.45 V vs. RHE after 12 h in 0.5 M glycerol in different pH solutions; (c) AuPt (15% Ptsurf) with applied potential of 0.45 V vs. RHE after 12 h in 1 M KOH in different glycerol concentration solutions; (d) AuPt (15% Ptsurf) with applied potential of 0.45 V vs. RHE in 0.5 M glycerol & 1 M KOH solution in 12 h.

explain the obvious difference of LA selectivity between Pt nanoparticle electrodes in this work and polycrystalline Pt electrodes previously reported [18,30], the dehydration and rearrangement of GLAD/DHA is considered. The mechanism study of glycerol oxidation on polycrystalline Pt by Kwon et al. [18,30] was employing online techniques; however, the HPLC and NMR tests in this work were performed ex-situ. Since the GLAD/DHA evolves into LA and other products automatically in alkaline media through dehydration and rearrangement [14,18,26], GLAD/DHA is observed by in-situ techniques, while LA is detected by ex-situ techniques. As a result, the LA selectivity of Pt nanoparticle electrodes in this work is different compared with previous report using polycrystalline Pt electrodes.

3.4. Influence of electrolyte pH, glycerol concentration and reaction time

The presence of a higher base concentration is expected to have a positive effect on glycerol conversion. The base deprotonates glycerol, and the alkoxide produced after the abstraction of H_α is a much more reactive species than the glycerol, hence a higher pH is considered to facilitate the catalytic performance (mainly the slower first deprotonation step) in metal catalyzed oxidation reactions [34–36]. The glycerol oxidation was performed using the AuPt (15% Pt_{surf}) catalyst in 0.5 M glycerol solution with KOH concentration from 0.1 M to 2 M. The glycerol conversion was 0.039 ± 0.001, 0.147 ± 0.010, 0.295 ± 0.018 and 0.307 ± 0.023 in 0.1, 0.5, 1, and 2 M KOH solution, respectively (shown in Fig. 6b), and the corresponding Faradaic current charges were 70, 194, 376, and 429 C, respectively. This is consistent with the trend in LSV results shown in Fig. 2b. The addition of base also enhanced the LA selectivity significantly when comparing the LA selectivity in 0.1 M KOH (39% LA) and 0.5 M KOH solutions (68% LA). This is in line with the proposed reaction pathways, where LA formation from GLAD/DHA is catalyzed by a base, whereas the subsequent oxidation of glyceraldehyde is a metal catalyzed oxidation reaction. Nevertheless, the LA selectivity changed insignificantly when the KOH concentration was higher than 0.5 M. This result indicates a relatively stable catalysis selectivity over limited pH change at high pH range.

The influence of glycerol concentration on the catalyst selectivity was also investigated. Fig. 6c demonstrates the production distribution of glycerol oxidation in 1 M KOH solution catalyzed by AuPt (15% Pt_{surf}) with glycerol of 0.05, 0.1, 0.5 and 1 M. The LA selectivity was approximately the same for all glycerol concentrations, suggesting a unique LA selectivity despite of the glycerol concentration. Additionally, the glycerol conversion declined from 0.582 ± 0.036 with 0.1 M glycerol to 0.154 ± 0.010 with 1 M glycerol. Product selectivity and glycerol conversion for the glycerol oxidation reaction in 0.5 M glycerol & 1 M KOH solution catalyzed by AuPt (15% Pt_{surf}) at 1, 2, 4, 6, and 12 h are shown in Fig. 6d. The product distribution remained relative constant after 1 h, while the glycerol conversion kept increasing in 12 h, from 0.068 ± 0.009 at 1 h to 0.295 ± 0.018 at 12 h. These results suggest that the stable selectivity of the catalysts towards reaction time during this particular period.

The total Faradaic efficiency of glycerol oxidation in 1 M KOH solution after 12-h reaction declined gradually from 0.871 in 0.05 M glycerol to 0.840 in 1 M glycerol, and the total Faradaic efficiency of glycerol oxidation in 0.5 M glycerol and 1 M KOH declined gradually from 0.994 at 1 h to 0.858 at 12 h (detailed in Table S2). To explain the decrease in the total Faradaic efficiency, the adsorption/desorption of reactant/intermediates/products, which is a non-Faradaic process, is discussed. It is reported that GA and TA, which consist of β-dicarbonyl structures, ultimately adsorb onto the metal surfaces and thus blocking the active sites for the glycerol oxidation reaction [25,41]. Hence, glycerol oxidation, which is a Faradaic process, is inhibited and leads to a lower Faradaic efficiency. At increasing glycerol concentration or reaction time, the oxidation products accumulate and the metal surfaces become increasingly populated by GA and TA. Consequently, the Faradaic efficiency decreases with the increasing glycerol concentration or reaction time.

In order to study the repeatability of the catalyst, the electrochemical characterization of AuPt nanoparticles before and after the chronoamperometry test. Fig. S6 shows the cyclic voltammograms of AuPt catalyst (15% Pt_{surf}) in 0.5 H_2SO_4 before and after the chronoamperometry performed at 0.45 V vs. RHE in 0.5 M glycerol and 1 M KOH for 12 h (optimal condition for LA production). It can be found that the change is minimal, and the surface Pt composition change from 13.2% to 14.0%. These results confirm the catalyst's recyclability and robustness under the optimal experimental condition for LA production.

4. Conclusion

In this paper, we report the electrochemical production of lactic acid from glycerol at room temperature and pressure. The selectivity for lactic acid can be achieved >70% on AuPt nanoparticles with a controlled surface composition. Lower oxidation potentials promoted the formation of lactic acid, and the Pt-enriched AuPt bimetallic catalyst showed an optimal performance, with the highest lactic acid selectivity and glycerol conversion. Additionally, the glycerol conversion was found to be tunable by varying the electrolyte pH, glycerol concentration, and reaction time, in addition to the applied potential and catalyst surface composition.

Acknowledgement

The authors acknowledge the financial support from the Campus for Research Excellence and Technological Enterprise (CREATE) in Singapore and Singapore Ministry of Education Tier 1 Grants (RG131/14 & RG18/16). The authors also acknowledge Facility for Analysis, Characterisation, Testing and Simulation (FACTS) in Nanyang Technological University for materials characterization.

Appendix A. Supplementary material

Supplementary data associated with this article can be found, in the online version, at https://doi.org/10.1016/j.jcat.2017.10.010.

References

[1] R.E. Drumright, P.R. Gruber, D.E. Henton, Polylactic acid technology, Adv. Mater. 12 (2000) 1841–1846.
[2] L.S. Sharninghausen, J. Campos, M.G. Manas, R.H. Crabtree, Efficient selective and atom economic catalytic conversion of glycerol to lactic acid, Nat. Commun. 5 (2014) 5084–5092.
[3] Y. Li, S. Chen, J. Xu, H. Zhang, Y. Zhao, Y. Wang, Z. Liu, Ni promoted Pt and Pd catalysts for glycerol oxidation to lactic acid, Clean Soil Air Water 42 (2014) 1140–1144.
[4] M. Morales, P.Y. Dapsens, I. Giovinazzo, J. Witte, C. Mondelli, S. Papadokonstantakis, K. Hungerbühler, J. Pérez-Ramírez, Environmental and economic assessment of lactic acid production from glycerol using cascade bio- and chemocatalysis, Energy Environ. Sci. 8 (2015) 558–567.
[5] M.A. Abdel-Rahman, Y. Tashiro, K. Sonomoto, Recent advances in lactic acid production by microbial fermentation processes, Biotechnol. Adv. 31 (2013) 877–902.
[6] S.S. Yazadani, R. Gonzales, Anaerobic fermentation of glycerol: a path to economic viability for the biofuels industry, Curr. Opin. Biotechnol. 18 (2007) 213–219.
[7] C.A.G. Quispe, C.J.R. Coronado, J.A. Carvalho Jr., Glycerol: Production, consumption, prices, characterization and new trends in combustion, Renew. Sust. Energy Rev. 27 (2013) 475–493.
[8] Glycerol Market Size, Price Trend, Research Report 2022, 2015.
[9] R. Ciriminna, C.D. Pina, M. Pagliaro, Understanding the glycerol market, Eur. J. Lipid Sci. Technol. 116 (2014) 1432–1439.
[10] H. Kishida, F. Jin, Z. Zhou, T. Moriya, H. Enomoto, Conversion of glycerin into lactic acid by alkaline hydrothermal reaction, Chem. Lett. 34 (2005) 1560–1561.
[11] H. Enomoto, F. Jin, T. Moriya, K. Kakeda, Y. Sekiguchi, H. Kishida, U.S. Patent 7,829,740 B2, 2010.
[12] Y. Shen, S. Zhang, H. Li, Y. Ren, H. Liu, Efficient synthesis of lactic acid by aerobic oxidation of glycerol on Au–Pt/TiO_2 catalysts, Chem. Eur. J. 16 (2010) 7368–7371.
[13] R.K.P. Purushothaman, J.v. Haveren, D.S.v. Es, I. Melián-Cabrera, J.D. Meeldijk, H.J. Heeres, An efficient one pot conversion of glycerol to lactic acid using bimetallic gold-platinum catalysts on a nanocrystalline CeO_2 support, Appl. Catal. B Environ. 147 (2014) 92–100.
[14] C. Zhang, T. Wang, X. Liu, Y. Ding, Selective oxidation of glycerol to lactic acid over activated carbon supported Pt catalyst in alkaline solution, Chin. J. Catal. 37 (2016) 502–509.
[15] R.V. Chaudhari, B. Subramaniam, D.S. Roy, Catalyst System and Process for Converting Glycerol to Lactic Acid, US, 2012.
[16] E.P. Maris, R.J. Davis, Hydrogenolysis of glycerol over carbon-supported Ru and Pt catalysts, J. Catal. 249 (2007) 328–337.
[17] J.T. Dam, F. Kapteijn, K. Djanashvili, U. Hanefeld, Tuning selectivity of Pt/$CaCO_3$ in glycerol hydrogenolysis — a design of experiments approach, Catal. Commun. 13 (2011) 1–5.
[18] Y. Kwon, K.J.P. Schouten, M.T.M. Koper, Mechanism of the catalytic oxidation of glycerol on polycrystalline gold and platinum electrodes, ChemCatChem 3 (2011) 1176–1185.
[19] Y. Kwon, Y. Birdja, I. Spanos, R. Paramaconi, M.T.M. Koper, Highly selective electro-oxidation of glycerol to dihydroxyacetone on platinum in the presence of bismuth, ACS Catal. 2 (2012) 759–764.
[20] S. Lux, P. Stehring, M. Siebenhofer, Lactic acid production as a new approach for exploitation of glycerol, Sep. Sci. Technol. 45 (2010) 1921–1927.
[21] H. Wang, L. Thia, N. Li, X. Ge, Z. Liu, X. Wang, Selective electro-oxidation of glycerol over Au supported on extended poly(4-vinylpyridine) functionalized graphene, Appl. Catal. B Environ. 166–167 (2015) 25–31.
[22] S. Sun, L. Sun, S. Xi, Y. Du, M.U.A. Prathap, Z. Wang, Q. Zhang, A.C. Fisher, Z. Xu, Electrochemical oxidation of C3 saturated alcohols on Co_3O_4 in alkaline, Electrochim. Acta 228 (2017) 183–194.
[23] M. Simões, S. Baranton, C. Coutanceau, Electrochemical valorisation of glycerol, ChemSusChem 55 (2012) 2106–2124.
[24] L. Roquet, E.M. Belgsir, J.M. Léger, C. Lamy, Kinetics and mechanisms of the electrocatalytic oxidation of glycerol as investigated by chromatographic analysis of the reaction products: Potential and pH effects, Electrochim. Acta 39 (1994) 2387–2394.
[25] J. Qi, L. Xin, D.J. Chadderdon, Y. Qiu, Y. Jiang, N. Beniqal, C. Liang, W. Li, Electrocatalytic selective oxidation of glycerol to tartronate on Au/C anode catalysts in anion exchange membrane fuel cells with electricity cogeneration, Appl. Catal. B Environ. 154–155 (2014) 360–368.
[26] C.H. Lam, A.J. Bloomfield, P.T. Anastas, A switchable route to valuable commodity chemicals from glycerol via electrocatalytic oxidation with an earth abundant metal oxidation catalyst, Green Chem. 19 (2017) 1958–1968.
[27] S.L. Gaw, J. Wang, S. Sun, Z. Dong, M. Reches, P.S. Lee, Z.J. Xu, Electrochemical cycling induced surface segregation of AuPt nanoparticles in $HClO_4$ and H_2SO_4, J. Electrochem. Soc. 163 (2016) F752–F760.
[28] J. Suntivich, Z. Xu, C.E. Carlton, J. Kim, B. Han, S.W. Lee, N. Bonnet, N. Marzari, L. F. Allard, H.A. Gasteiger, K. Hamad-Schifferli, Y. Shao-Horn, Surface composition tuning of Au–Pt bimetallic nanoparticles for enhanced carbon monoxide and methanol electro-oxidation, J. Am. Chem. Soc. 135 (2013) 7985–7991.
[29] D. Padayachee, V. Golovko, B. Ingham, A.T. Marshall, Influence of particle size on the electrocatalytic oxidation of glycerol over carbon-supported gold nanoparticles, Electrochim. Acta 120 (2014) 398–407.
[30] Z. Wang, L. Xin, X. Zhao, Y. Qiu, Z. Zhang, O.A. Baturina, W. Li, Carbon supported Ag nanoparticles with different particle size as cathode catalysts for anion exchange membrane direct glycerol fuel cells, Renew. Energy 62 (2014) 556–562.
[31] S. Cherevko, A.R. Zeradjanin, G.P. Keeley, K.J.J. Mayrhofer, A comparative study on gold and platinum dissolution in acid and alkaline media, J. Electrochem. Soc. 161 (2014) H822–H830.
[32] Y. Kwon, M.T.M. Koper, Combining voltammetry with HPLC: application to electro-oxidation of glycerol, Anal. Chem. 82 (2010) 5420–5424.
[33] C.S. Carlson, J.P.V. Smith, U.S. Patent 2,614,072 A, 1952.
[34] B.N. Zope, D.D. Hibbitts, M. Neurock, R.J. Davis, Reactivity of the gold/water interface during selective oxidation catalysis, Science 330 (2010) 74–78.
[35] Y. Kwon, S.C.S. Lai, P. Rodriguez, M.T.M. Koper, Electrocatalytic oxidation of alcohols on gold in alkaline media: base or gold catalysis?, J Am. Chem. Soc. 133 (2011) 6914–6917.
[36] P. Rodriguez, Y. Kwon, M.T.M. Koper, The promoting effect of adsorbed carbon monoxide on the oxidation of alcohols on a gold catalyst, Nat. Chem. 4 (2012) 177–182.
[37] M. Pagliaro, R. Ciriminna, H. Kimura, M. Rossi, C.D. Pina, From glycerol to value-added products, Angew. Chem. Int. Ed. 46 (2007) 4434–4440.
[38] D. Mott, J. Luo, P.N. Njoki, Y. Lin, L. Wang, C.-J. Zhong, Synergistic activity of gold-platinum alloy nanoparticle catalysts, Catal. Today 122 (2007) 378–385.
[39] M.Ø. Pedersen, S. Helveg, A. Ruban, I. Stensgaard, E. Lægsgaard, J.K. Nørskov, F. Besenbacher, How a gold substrate can increase the reactivity of a Pt overlayer, Surf. Sci. 425 (1999) 395–409.
[40] J.F. Gomes, G. Tremiliosi-Filho, Spectroscopic studies of the glycerol electro-oxidation on polycrystalline Au and Pt surfaces in acidic and alkaline media, Electrocatalysis 2 (2011) 96–105.
[41] B.N. Zope, R.J. Davis, Inhibition of gold and platinum catalysts by reactive intermediates produced in the selective oxidation of alcohols in liquid water, Green Chem. 13 (2011) 3484–3491.